International Journal of Research in Engineering Sciences and Management
Vol.2, No.1, Jan-June' 2025
*E-ISSN: 3107-4383*

# Biosynthesis of ZnO Nanoparticles Using *Bombax ceiba* flower petals' extract and Investigation of their Photocatalytic and Biological Activities

Ravi Kant[1,2], Monika Chahar[1*], Anuj Mittal[2], Seema[3]
[1]*Department of Chemistry, Baba Mastnath University, Asthal Bohar, Rohtak (Haryana)*
[2]*Department of Chemistry, M.N.S. Government College, Bhiwani (Haryana)*
[3]*Department of Chemistry, University of Rajasthan, Jaipur, 302004*
[*]Corresponding author email: chaharmonika507@gmail.com

**Abstract:** Plant extract–mediated synthesis of zinc oxide nanoparticles (ZnO NPs) is an eco-friendly method that utilizes phytochemicals as natural reducing and stabilizing agents, to produce biocompatible and stablenanoparticles with tunable properties. This study reports the synthesis of ZnO Nanoparticles utilizing anaqueous extract of Bombax ceiba flower petals (BC). The characterization of BC-ZnO NPs was carried out using UV–visible (UV-Vis.), Powder XRD, FTIR, and FESEM-EDS spectroscopic methods. PXRD pattern confirms highly crystalline ZnONPs with a wurtzite hexagonal phase.The FESEM images revealed the flake-like or petal-shaped appearance of the particles, giving a flower-like or agglomerated granular morphology. BC-ZnO NPs with an average size ~41.89 nm were obtained. BC-ZnO NPs exhibited ~90% photodegradation of MB dye during initial 40 min of UV light irradiation. Further, the BC-ZnO NPs were also examined for their biological activities: antimicrobial, antioxidant, and antidiabetic. BC-ZnO NPs showed excellent antioxidant capability and good antimicrobial potential against *C. albicans*, *S. aureus*, and *E. coli*. They showed better antidiabetic activity (α-amylase activity) than the standard, with an $IC_{50}$ value of 119.95 µg/mL. While for α-glucosidase, the BC-ZnO NPs exhibited excellent inhibition activity achievingan $IC_{50}$ value of 98.94 µg/mL.The lower $IC_{50}$ value (46.34 µg/mL) of the synthesized NPs was represented as their excellent antioxidant capability.

**Keywords:** Green Synthesis; *Bombax ceiba* flowers; Crystalline; Photocatalysis; Anti-diabetic; Antimicrobial

## 1. Introduction

In light of growing water scarcity, the efficient management and treatment of wastewater have become vital for the sustainability of emerging economies. Various industriesincluding textiles,

pharmaceuticals, leather, and printingcontinue to discharge substantial volumes of untreated effluent, posing serious health risks to public and environmental health[1, 2]. To address this, there is an urgent need for affordable yet highly effective wastewater treatment solutions. Among the emerging strategies, nanomaterials have receivedplenty ofattentionbecause of their distinctive features and promising performance in advanced treatment technologies[3–5]. Consequently, photocatalysis serves as an essential technique for applications involving energy storage and pollution degradation[6]. Semiconducting metal oxides,including $TiO_2$, ZnO, $WO_3$, CuO, and $SnO_2$, are commonly employed as photocatalysts to enhance electrochemical processes in energy conversion applications and to facilitatethe breakdown of pollutants in water treatment methods[5]. Nanomaterials, including nanoparticles (NPs) and nanorods (NRs), have been the focus of extensive research in recent decades due to their remarkable physical and chemical characteristics[7].

Further, as infections and bacteria are becoming more resistant to antibiotics, it is necessary to create new substances that can kill the microorganism without increasing the likelihood that adaptations will develop.Therefore, it is imperative to produce novel components with antibacterial capabilities. ZnO NPs have drawn more interest recently as an antimicrobial agent, thanks to their greater surface area which greatly assists the interaction with microorganisms. High binding energy (60 meV), direct broad band gap (3.02–3.30 eV), high melting point (1975 $^{\circ}C$) and n-type semiconducting nature, makes it a potential candidate for the versatile applications. According to many studies, ZnO NPs have a low impact on human cells but exhibit specific toxicity to certain bacteria[8, 9].The antibacterial properties of ceramics like ZnO have been thoroughly investigated by researchers in the last 10 years to replace traditional organic powder to cure various ailments. Since mineral components like zinc are necessary for human health and can have potent antibacterial properties even in the absence of sunshine, metal oxides like ZnO are favored over traditional organic powders[10]. By regulating and altering the parameters used during ZnO synthesis, it is possible to tailor the particle size, shape, and porosity of ZnO and enhance its performance[11].

Researchers are attempting to use green chemistry, or a green method, to lessen the issues related to hazardous chemicals. Nanoparticles produced through green synthesis offer advantages over traditional physicochemical methods and are well-suited for biomedical applications owing to

their distinctive and enhanced properties[12, 13]. This eco-friendly approach utilizes various biological sources, including plant extracts, microbial organisms (such as bacteria, algae, and fungi), and natural templates for synthesis[13, 14]. The plant extracts used in green synthesis contain a variety of phytochemicals that not only facilitate the synthesis of nanoparticles but also contribute to the formation of surface coatings[13, 15, 16]and prevent nanoparticle aggregation, thereby enhancing their stability and prolonging their lifespan in *in vivo* conditions when compared to nanoparticles synthesized through conventional methods[17].

Saha et al. utilized *Swertia chirayita* plant extract to synthesize ZnO NPs through different techniques. The produced ZnO NPs exhibited improved photocatalytic activity (88.67%), a reduced particle size (17 nm), and better antibacterial activity against *S. aureus* (28 mm) and *E. coli* (26 mm)[10].Negash et al. attempted to create reduced graphene oxide-zinc oxide (rGO@ZnO) nanocomposites utilizing *C. macrostachyus* leaf extract in an environmentally benign manner. These NPs caused 99 % photodegradation of MB dye in 100 minutes[18].Kant et al. successfully prepared green ZnO NPs using white ash gourd fruit extract.They achieved 80% photodegradation efficiency against MB dye in 30 minutes and 99% in 90 minutes of UV light irradiation. Further, these NPs were shown to exhibit excellent antidiabetic activity compared to standard, moderate antimicrobial activity and better antioxidant capability[19].

Among the different plants used in green synthesis, *Bombax ceiba* is a wild deciduous tree belonging to the Bombacaceae family[20–22],native to Asia and widely distributed across temperate and tropical regions of Asia, Africa, and Australia[23]. It is known by various vernacular names, including Semal, Silk-cotton tree (English), etc. Multiple parts of the plant, particularly its flowers, have long been used in traditional medicine for treating ailments such as wounds, gastrointestinal disorders, and as an expectorant, owing to its rich phytochemical profile[24].The flowers are reported to exhibit diuretic, laxative, tonic, and restorative effects due to their bioactive compounds[20]. These effects are attributed to phytochemicals like flavonoids, terpenoids, saponins, carbohydrates, tannins, and glycosides, which also contribute functional surface groups during nanoparticle synthesis[25]. Qualitative phytochemical screening of *B. ceiba* flower water extracts has revealed the presence of carbohydrates, triterpenoid sterols, glycosides, flavonoids, alkaloids, quinones, saponins, and tannins[26–28]. Studies suggest these

phytoconstituents are crucial in reducing metal ions to the nanoscale and stabilizing the resulting nanoparticles[17].

In keeping with this pattern, this study describes a sustainable production of ZnO NPs utilizing an extract from *Bombax ceiba* flower petals, their characterization and utilization towards pollutant removal and biological applications.

## 2. Materials and methods

### 2.1. Materials

Zinc acetate dihydrate, sodium hydroxide, double-distilled water, and ethanol were purchased from Sigma Aldrich. Every chemical and reagent were of analytical grade and utilized as such (no other purification).

### 2.2. Preparation of *Bombax ceiba* flower petals extract

Collected*Bombax ceiba* flowersin February. The flower petals were first washed and rinsed using tap water and then with distilled water. Petals were dried in a dark room. Then, put the dry petals inside a blender to be crushed and make a fine powder. Took 10 g of this dry powder in a conical flask and added 100 mL of distilled water. After that, themixture was heated in a water bath at 80$^{o}$C for 20 minutes. Cooled the solution and filtered it with Whatman filter paper. Filtrate with a brownish copper color was produced and utilized for the green synthesis of ZnO NPs.

### 2.3. Biosynthesis of ZnO NPs using *Bombax ceiba* flower petals' extract

5 g of zinc acetate dihydrate was dispersed in 50 mL of water in a beaker, then added aqueous extract of *B. ceiba* flower petalsand the mixture was stirred continuously for 45 min at room temperature. The pH was then gradually adjusted to 10through the dropwise addition of 2N NaOH solution while maintaining constant stirring. It was persistently stirred for 60 min at 80$^{o}$C. Dark creamy white precipitateappeared.The precipitate was cooled down, filtered, and subsequently washed thrice with double distilled water and twice with ethanol. Driedthe precipitates in an oven by heating for 4h at 85$^{o}$C. Consequently, an off-white-colored powdered form was produced, which was utilized for additional testing and characterization. The synthesis process for ZnO NPs using plant extract is schematically shown in Fig.1

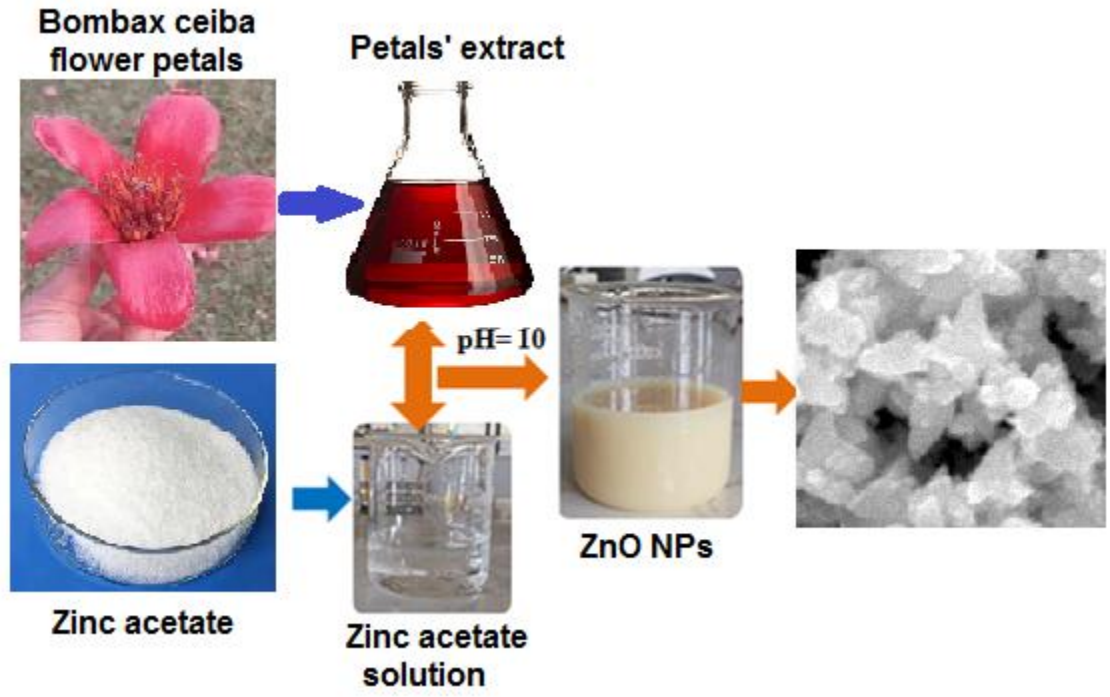


**Fig.1** Schematic illustration of the synthesis of BC-ZnO NPs

### 2.4. Characterization

The prepared ZnO NPs were characterized by UV–Visible, FTIR, Powder XRD, FE-SEM, and EDS techniques. Using a Perkin Elmer spectrophotometer (Lambda-750), the UV–Vis absorption spectrum was measured in the 200-800 nm range for evaluation of optical features and band gap calculation. The presence of different (functional) groups was certified by acquiring the spectrum using an FTIR spectrophotometer (PerkinElmer) within the range of 4000–400 $cm^{-1}$ using KBr pellets. The sample's XRD pattern was taken by an X-ray diffractometer (Panalytical X Pert Pro). It was carried out between 2 theta range of 10 to 80° in 2°/min steps to examine the crystallinity and phase purity of prepared ZnO NPs. An analysis of the sample's surface morphology was conducted by FESEM (Nova Nano 450-FEI), and elemental composition was established through the EDS investigation.

### 2.5. Photocatalytic study

To calculate the photodegradation efficiency of the sample, the decolorization of Methylene Blue (MB) dye under UV light irradiation was used. The MB dye solution taken for the study was 150 mL of 5 ppm. The adsorption-desorption equilibrium was established by dispersing the ZnO NPs (50 mg) in MB dye solution (150 mL) and stirring it for an hour without light. The mixture was put into a double-jacketed photocatalytic reactor that had a magnetic stirrer and a 250 W xenon

lamp installed. The system was kept at the proper temperature by means of water circulation. The right amount of the mixture was collected at various times and centrifuged to separate the catalyst. By determining the absorbance of supernatant liquid using a UV–Visible spectrophotometer, the dye concentration was assessed. The following formula was used to get the dye degradation rates:

$$\text{Degradation efficiency} = \frac{C_0 - C_t}{C_0} x100$$

where Co is the initial concentration of dye after adsorption-desorption equilibrium, and $C_t$is the concentration at a definite time.

The kinetics of photodegradation of MB dye over ZnO NPs examined by employing the given equation:ln ($C_t/C_o$) = -kt,

where $C_o$denotes initial concentration, $C_t$, concentration at t time, and k is rate constant. Plotting the – ln($C_t/C_0$) against time (t) yielded a straight line whose slope indicated the rate constant of the photodegradation[30, 31].

**2.6.Biological activity**

**2.6.1. Antimicrobial activity**

Using Agar Well-Diffusion method, the antimicrobial potential of the synthesized ZnO NPs was evaluated against *S. aureus*, *E. coli* (bacterial strains), and *C. albicans* (fungal strain). Mueller Hinton agar no. 2 (Hi-Media, India) and Sabouraud's dextrose agar (SDA) were used as the bacteriological and fungal medium, respectively. The microbes' culture was prepared using agar media. Sterilized filter paper discs soaked in various concentrations of ZnO NPs (20 µL, 40 µL, 60 µL, and 80 µL) were placed on agar plates to assess the antibacterial activity. Then strains of *S. aureus*, *E. coli*, and *C. albicans* were incorporated into agar plates. Filter paper discs containing Ketoconazole (for fungal strains) and Ciprofloxacin (for bacterial strains) were also added to agar plates as positive control medications to compare antibacterial activity. For antibacterial studies, the loaded agar plates were incubated at 37 °C for 24 h while for antifungal evaluation, incubation was carried out at 28 °C for 48 h. Finally, the zone of inhibition around the filter paper disc was measured to assess the antibacterial potency of the synthesized ZnO NPs. Every experiment was run three times[32].

**2.6.2. Antioxidant activity**

The prepared ZnO NPs were assessed for their antioxidant potency through the DPPH assay,

which is primarily used to investigate the nanomaterial's capacity to scavenge radicals[33]. The antioxidant potential of green-preparedZnO NPs was investigated via DPPH assay by increasing their concentration from 20 mg/mL to 100 mg/mL across the two samples. 1 mL of ZnO NPs sample in methanol mixed with 1 mL of DPPH. In the standard experiment, 1mL of standard ascorbic acid was combined with 1 mL of DPPH which acted as a reference for antioxidants. The ZnO NPs samples and standard were incubated at 37$^{o}$C for 30 min. Methanol was used as a blank. All sample color changes were tracked, and the sample's absorbance was assessed using UV–Visible spectroscopy with a maximum wavelength of 517 nm. For every sample, the values were taken in triplicate. The ability of synthesized ZnO NPs to scavenge free radicals (%) was assessed as follows:

Blank – methanol and Control – methanol + DPPH (1:1)

$$\%\ \text{DPPH scavenging activity} = \frac{A_c - A_s}{A_c} x100$$

Where $A_C$ = absorbance of DPPH control, and $A_S$ = absorbance in the presence of the test sample.

### 2.6.3. Antidiabetic activity

Synthesized ZnO NPs' antidiabetic potential was evaluated using 500 µg/mL concentrations. The antidiabetic potency was assessed in *in vitro* α-amylase and α-glucosidase enzyme inhibition assay, and Acarbose was utilized as a standard[34].

**α- amylase assay-** By employing the DNS method, α-amylase action was assessed. A mixture was prepared by combining 500 µg of synthesized ZnO sample, 500 µL of 0.02 M $Na_3PO_4$ buffer solutioncontaining6 mM NaCl, and 0.04 units of α-amylase. This prepared mixture solution of ZnO NPs was then incubated at 37°Cfor 10 minutes. Following incubation, 500 µL of 1% starch solution was added to initiate the reaction. To cease the reaction,1.0 mL of 3,5-Dinitrosalicylic acid (DNS) reagent was introduced. The test tubes were placed in a boiling water bath for five minutes and then cooled down to room temperature. Lastly, the reaction mixture was diluted using 10mL of distilled water, and its absorbance was noted at 540 nm.

**α-glucosidase assay-** For five minutes, the 500µg ZnO sample was incubated at 37°C with 0.2 M Tris buffer (pH 8.0) and 1 mL of the 2% starch substrate solution. To initiate the reaction, 1 mL of α-glucosidase enzyme (1µg/mL) was added to the mixture, followed by incubation at 35°C for 40 min. The reaction was subsequently terminated by the addition of 2 cc of 6N HCl.

The color intensity was then estimated by measuring the absorbance at 540 nm. Likewise, the control samples were readied without the nanoparticles of green synthesized ZnO. The percentage of enzyme inhibition and the $IC_{50}$ value were determined. Percent inhibition was calculated to estimate the activity using the formula:

$$I = \{(Abs_{Control} - Abs_{Sample})/Abs_{Control}\}x100$$

## 3. Results and Discussion

### 3.1. UV–Visible analysis

The BC-ZnO NPs' UV-visible spectrum was taken to examine their absorbance and bandgap. It is shown in Fig.2 (a).There's a sharp increase in absorbance between 350–380 nm, peaking near 356 nm, followed by a steep drop-off. The absorbance starts high (~1.0) and gradually increases before the absorption edge. This is typical for ZnO nanoparticlesdue to excitonic absorption in the UV region. After ~400 nm, absorbance declines and remains low, which is consistent with ZnO being a widebandgap semiconductor[35, 36]. The absorption edge around 356 nm corresponds to the band gap energy ~ 3.48 eV (Using the formula[37]: Eg=hc/λ=1239.8/λ(nm); For λ = 356 nm, Eg = 1239.8/356 = 3.48 eV). This is typical for ZnO, whose bulk bandgap is ~3.3 eV[38]. A slight blueshift from this value may indicate quantum confinement in small nanoparticles. Shifting to shorter wavelengths (higher energy) suggests smaller particle sizes[37]. The clean, sharp absorption edge without extra peaks suggests good crystallinity, few surface defects or impurities and minimal presence of secondary phases.

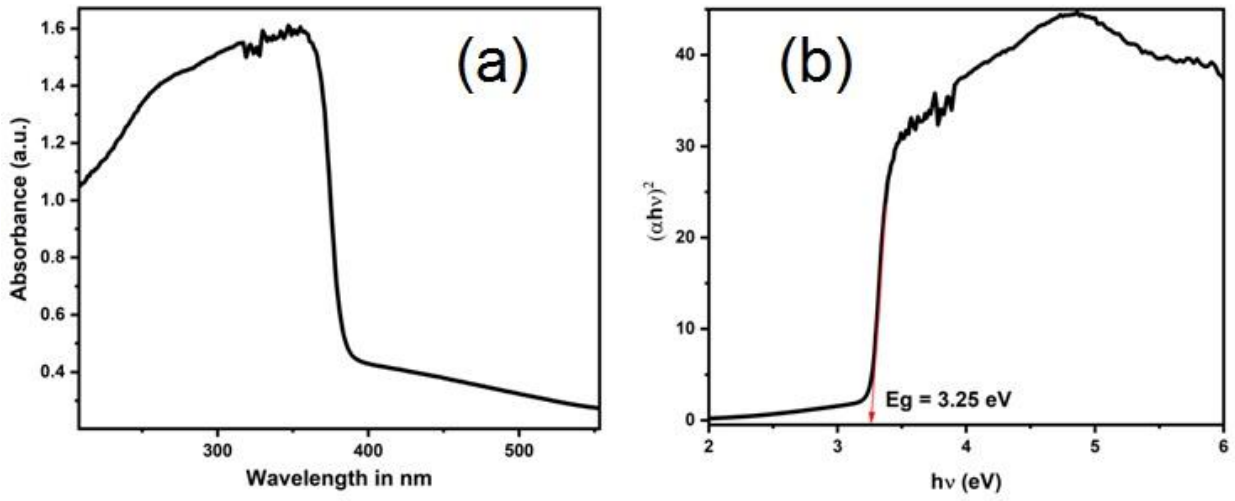


**Fig. 2** (a) UV–visible spectra (b) Tauc plot for BCF-ZnO NPs

Value of $E_g$ is also estimated using Tauc Equation: $(\alpha h\nu)^{1/n} = K (E_p-E_g)$, where the symbolsα, h,ν, $E_p$, and $E_g$, respectively denote absorption coefficient, Planck's constant, frequency of the incident photon,the photon energy (hν), andthe optical band gap. K and n are constants wherethe value of nis decided on the basis of kind of electronic transition: ½ for allowed direct, 2 for allowed indirect, 3/2 for forbidden direct, and 3 for forbidden, indirect transitions[39]. For ZnO, which typically exhibits a direct allowed transition, n = ½, so $(\alpha h\nu)^2$ is plotted versus hvand extrapolating the linear region of the plot to $(\alpha h\nu)^2= 0$, will provide the value of $E_g$[40]. The estimated Eg for the BC-ZnO is 3.25 eV (Fig.2 (b)).

**3.2. XRD investigation**:

Each crystalline substance has a unique diffraction pattern**.** By comparing the peak positions (2θ values) and their intensities with standard databases (like JCPDS), one can identify the crystalline phase(s) present.XRD pattern of the BCF-ZnO NPsis depicted in Fig.3.The major peaks appearing at specific 2θ values, are indexed in figure with corresponding Miller indices (hkl): ~31.7° (100) Wurtzite ZnO, ~34.4° (002) strong peak → preferred orientation, ~36.2° (101) most intense peak, ~47.5° (102) secondary peak, ~56.6° (110) minor, ~62.8° (103) minor, ~66.4° (200) minor, ~69.1° (201) minor. These diffraction peaks closely corresponds to the standard wurtzite hexagonal phase of ZnO (JCPDS card no. 36-1451), confirming: single-phase ZnO andno significant impurities or secondary phases (e.g., $Zn(OH)_2$ or Zn)[41, 42].Hence, the XRD pattern confirms high crystallinity (indicated byfirm and narrow peaks) of ZnOnanoparticles with a wurtzite hexagonal structure. No additional peaks from impurities are visible, indicating high purity. The sharp peaks, especially the intense (101), suggest well-formed crystalline domains[43, 44]**.**

The Debye–Scherrer formula highlights that smaller crystallitesproduce broader peaks in the XRD pattern, whereas larger crystallites result in narrower, sharper peaks. By analyzing the peak broadening, this equation enables the assessment of the average crystallite in a material. If we assume the (101) peak at ~36.2° as most intense, and the full width at half maximum (FWHM) is known, we can estimate the crystallite size (D) using the Debye-Scherrer equation:

$$D = \frac{K\lambda}{\beta cos\theta},$$

Here, D represents crystallite size in nanometers (nm), K represents Scherrer constant with a typical value of 0.9, and λ is the wavelength of the X-ray usedspecifically, Cu Kα radiation

(0.15046 nm). β represents FWHM of the most intense peak in the XRD pattern, typically observed at 2θ = 36.48° for the (101) plane, while θ is the Bragg angle obtained from the 2θ value.

The average size (D) of prepared ZnO NPs is found to be in the range of 41.89 nm.The particle size determines the cosmetic qualities of zinc oxide as a sunscreen; the smaller the particle size on the nanoscale (less than 100 nm), the greater the UV scattering capacity[45].

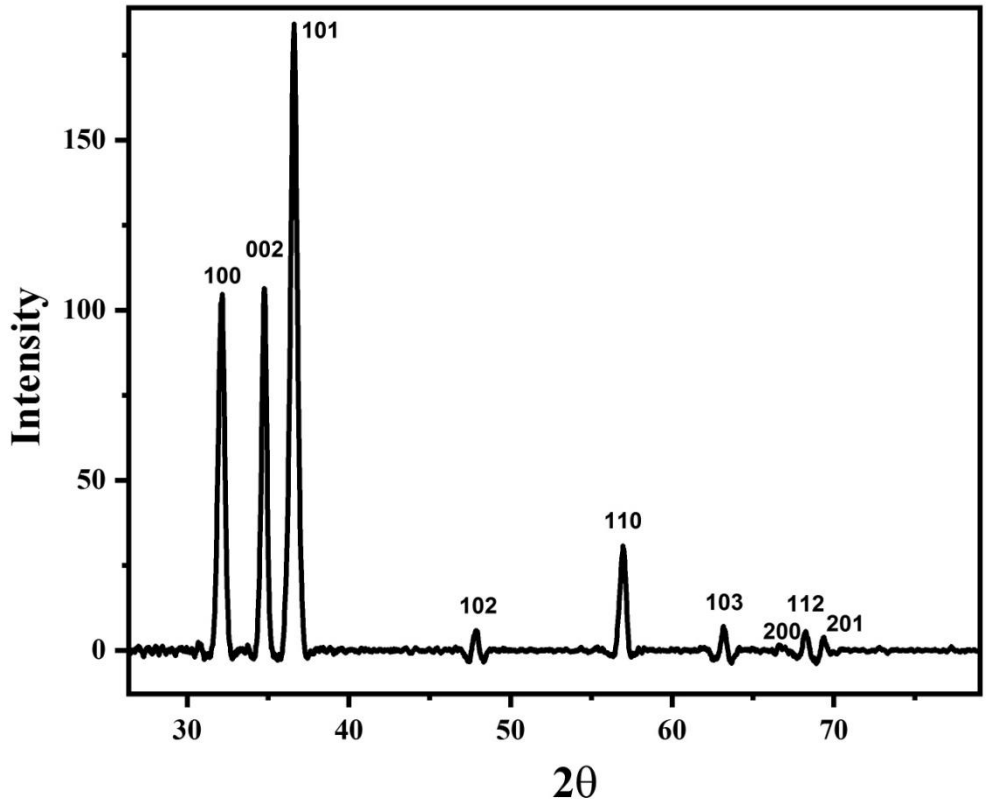


**Fig. 3** XRD plot of BC-ZnO NPs

### 3.3. FTIR analysis:

Fig.4presents the findings of the FTIR study and shows several functional groups' presence.The intense peaks at ~510 $cm^{-1}$ and 408 $cm^{-1}$are characteristic of Zn–O vibrations, confirming successful formation of ZnO NPs[46, 47]. The O–H band at 3744 $cm^{-1}$and bending at 1372 $cm^{-1}$imply surface-adsorbed water or hydroxyl groups and phenols in *Bombax ceiba* flowers' extract[48]. Peaks at 2960 $cm^{-1}$ (C–H) and 1744 $cm^{-1}$ (C=O) indicate residual organics' presence, which might be from plant extract.Bands at 1577 $cm^{-1}$ suggest C=C(may be aromatic rings or alkenes), 1214 $cm^{-1}$indicatesasymmetric stretch ofC–O(characteristic of polyphenolic

substances), and 882 $cm^{-1}$ may be due to C-H out-of-plane bending, indicative of aromatic structures. This supports the idea of organic molecules attached to or interacting with the ZnO surface[49].Presence of hydroxyl groups,organic compounds, and carbonyl functionalities indicates: surface capping, possibly stabilizing the particles and moisture absorption or surface interaction with atmospheric/environmental components.

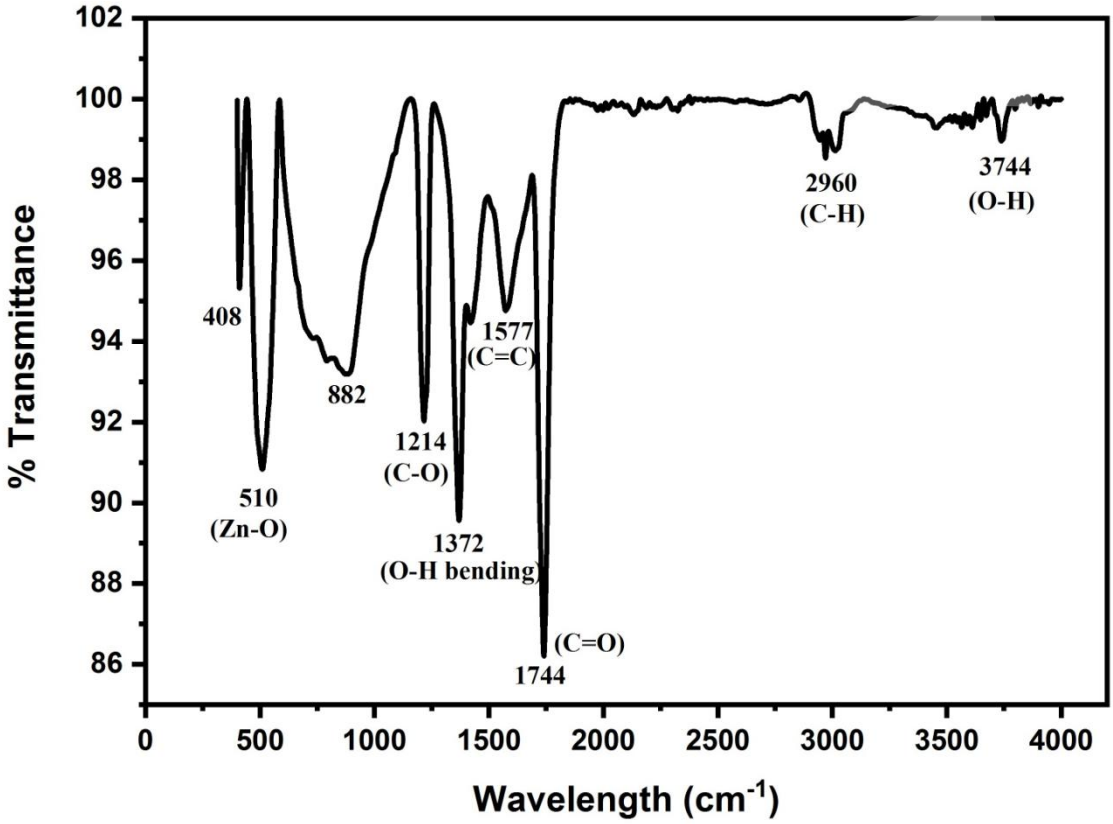


**Fig.4**FTIR of BC-ZnONPs.

### 3.4. FESEM analysis and EDS analysis:

The surface characteristics of BC-ZnO NPs were mainly assessed by the FESEM analysis. Through the study of surface roughness, SEM enables us to define the growth mode[50].From the SEM images (Fig.5) of the synthesized samples, it is evident that the material exhibits a highly textured, rough, and densely packed nanostructure. Particles are flake-like or petal-shaped, giving a flower-like or agglomerated granular morphology. Usually, because of its extended petal architecture, the ZnO nanoflower has a large surface area per unit volume. With Surface functionalization and modification, these nanoflowers can be employed in catalysis and biomedical applications. Previously, the ZnO nanoflower has been utilized in developing

biosensors and as a medicinal agent for numerous illnesses[51]. Similarly ZnO nanoflakes under UV light had demonstrated exceptional photocatalytic efficacy for dye degradation[52].

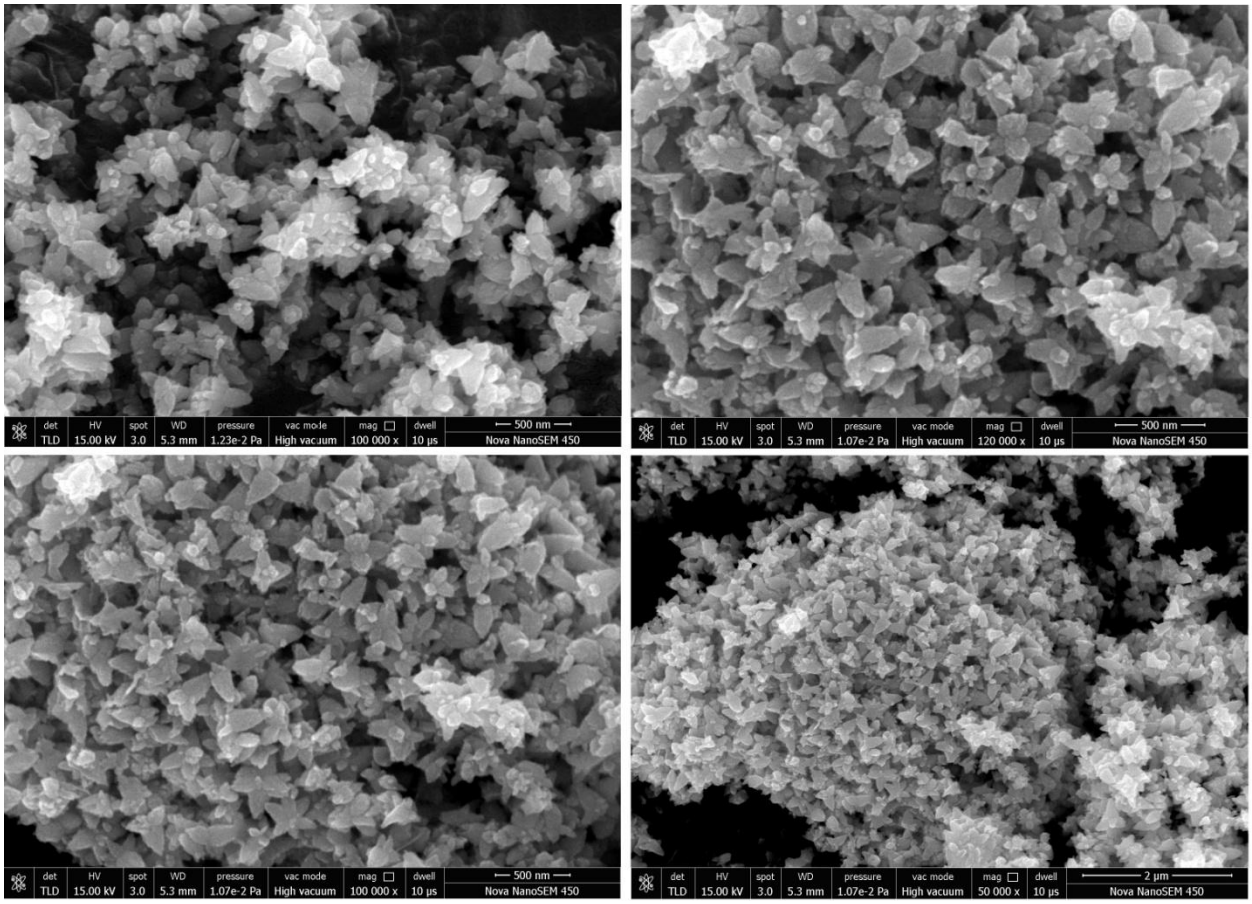


**Fig. 5**SEM images of the BC-ZnO NPs

In SEM images (Fig.5), the surface appears homogeneous at higher magnifications, with consistent formation across the field of view, suggesting uniform growth. The material shows inter-particle voids and mesoporous architecture visible as the dark regions between clusters. Pores appear irregular in shape and distribution, likely resulting from the random stacking and agglomeration of the flakes. These are interconnected, suggesting good permeability beneficial for applications like catalysis, sensors, or electrochemical electrodes. Slight agglomeration is noticeable, which is common in nanoscale materials.

EDS (Energy Dispersive X-ray Spectroscopy) is a method used to identify the elements within a sample and estimate their relative quantities. It operates by directing a beam of electrons onto the sample, which results in the emission of X-rays that are unique to the elements present. Fig.6 depicts the EDS spectrum of BC-ZnO sample, revealing the successful presence of Zn with a

smaller amount of oxygen. The spectrum is comprised of peaks corresponding to Zn (at 1.00 and 8.6 keV) and O (0.5 keV) only, confirming their purity. The chemical composition of reported ZnO NPs is exhibited in the table as shown in the inset of Fig.6. The EDS analysis revealed theweight percentages of Zn and O to be 98.44 % and 1.56 %, respectively, with corresponding atomic percentagesof 93.90 % and 6.10 %. Thesevalues deviate significantly from the theoretical stoichiometric weight percentages of Zn and O in ZnO, which are 80.34 % and 19.66 %, respectively.This notable deviation can beattributed to the presence of organic compounds derived from the phytochemicals of *B. ceiba* flower petals' extract used during synthesis.

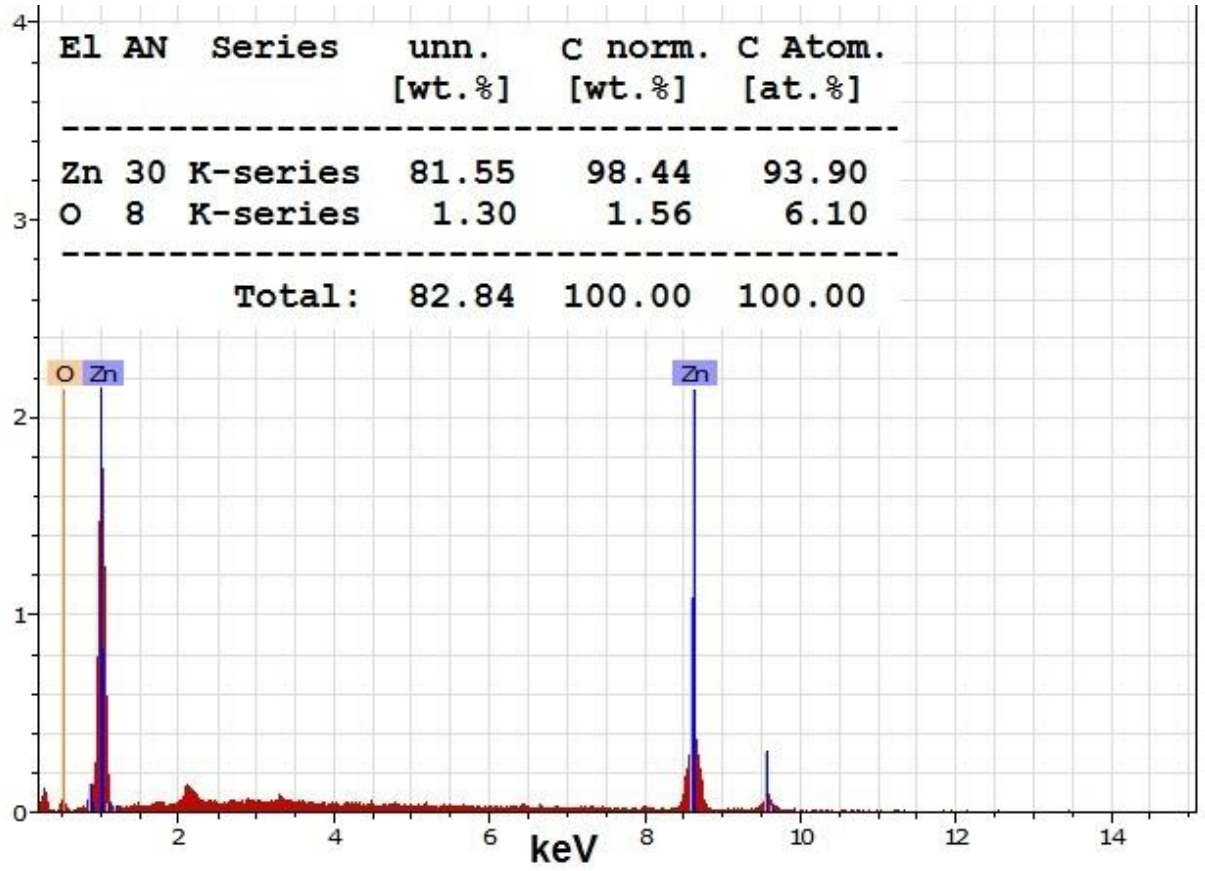


**Fig.6** EDS spectrumof the BC-ZnO NPs

These organic constituents may have lead to the formation of oxygen vacancies in the ZnO NPs; an advantageous property for photocatalytic applications.The oxygen vacancies (caused by Zn excess or O deficiency) may introduce defect states in the band gap which act as electron traps; reducing recombination of electron-hole pairs, thereby improve photocatalytic efficiency.Further, ZnO being popular for gas sensing capabilities, may get benefited with these

oxygen vacancies. The surface reactivity gets increased by oxygen vacancies; enabling faster and more sensitive interaction with gases. These vacancies act as active sites for gas adsorption, causing a change in conductivityand producing detectable signals for gas sensing in no time.Additionally, the absence of extra peak(s) in the EDS spectrum confirms the purity of theBC-ZnO NPs[53].

### 3.5. Photocatalytic analysis:

#### 3.5.1. Photodegradation of MB dye by BCF-ZnO NPs:

Fig.7 demonstrates the degradation of MB dye over BC-ZnO photocatalyst under UV light at room temperature for 110 min. The photodegradation is examined by noticing a substantial reduction of the maximum absorption peak's (at 663 nm) intensity (over time) in UV spectra (Fig.7).

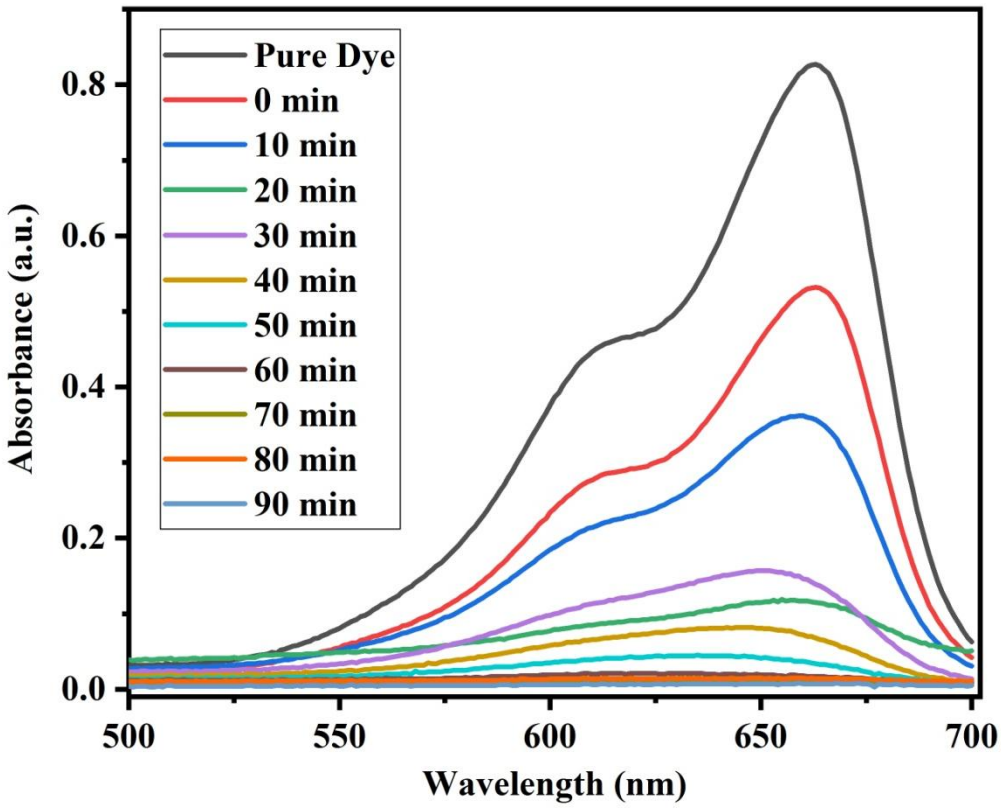


**Fig.7**UV spectra of the photodegradation of MB dye in the presence of BC-ZnO NPs

ZnO nanoparticles show strong photocatalytic degradation ability under irradiation. The steady decrease in absorbance at the dye's characteristic $\lambda_{max}$ (~663 nm) suggests efficient dye

degradation by ZnO NPs. The dye's absorbance intensitydecreases steadily, indicating continuous breakdown of chromophoric groups. At 90 minutes, the dye is nearly degraded, as shown by the drastically reduced absorbance. The complete decolorization by ~90 minutes confirms high degradation efficiency. Hence synthesized ZnO NPs can be considered a capable candidate for wastewater treatment and dye remediation.

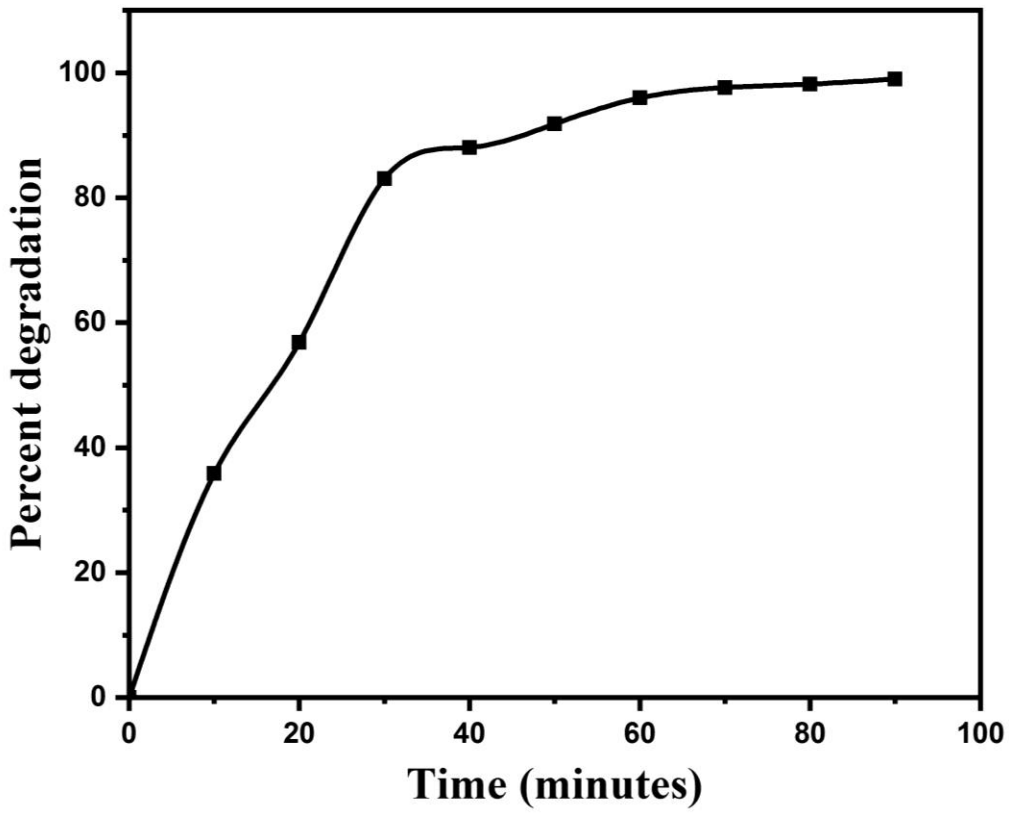


**Fig.8**Percent degradation of MB dye with time using BC-ZnO NPs

The prepared ZnO NPs exhibited excellent photocatalytic performance: 99% photodegradation efficiency against MB dye in 90 minutes of UV light irradiation (Fig.8 & 9). The degradation starts rapidly, reaching ~55% in 20 minutes, indicating high photocatalytic activity during the early stages due to abundant active sites and high dye concentration. After ~60 minutes, the curve begins to plateau, approaching maximum degradation (~98–99%). This slowing down is likely due to: depletion of dye molecules in the solution, saturation of active sites and accumulation of intermediate species on the catalyst surface.

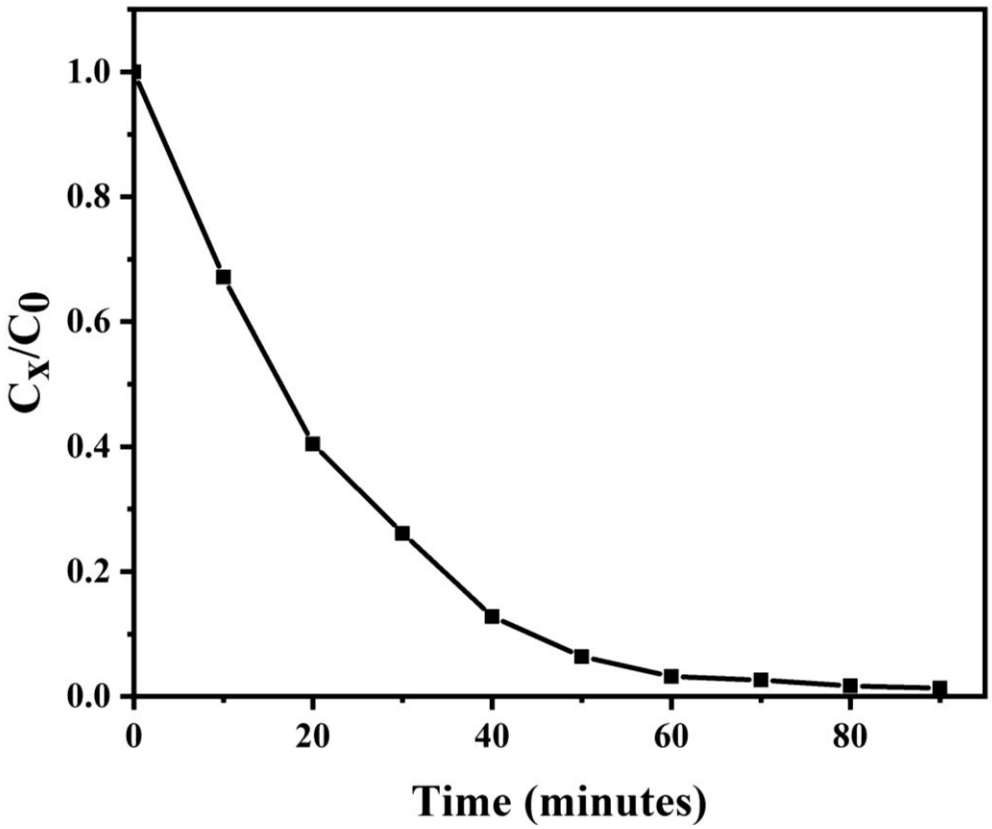


**Fig.9**Variation of relative concentration of MB with respect to time utilizing BCF-ZnONPs

The plot (fig.9) shows a rapid initial decrease in concentration followed by a slower decline, indicatingpseudo-first-order kinetics, typical for photocatalytic dye degradation. At ~40 minutes, the concentration drops to ~0.1 (i.e., almost 90% degradation).Over 95% degradation is achieved within 60 minutes, making this ZnO sample an essential material for dye removal in contaminated water.

**3.5.2.Kinetics of photo degradation:**

Kinetics of the degradation were studied by plotting -ln (*Cx*/*Co*) vs. time. Together with the rate constant, this graph (Fig.10) also provides the regression coefficient's value, which helps determine the degradation's kinetics and order. The graph is a straight line, with the regression constants' value above 0.98 and a comparatively greater rate constant, as listed in Table 1.

As per Fig.10, the photodegradation of MB dye over ZnO nano photocatalysts follows pseudo-first-order kinetics, and the equation ln ($C_t/C_0$) = -kt (pseudo-first-order eqn.)matches the experimental findings quite well[48, 54].

The value of rate constants (k) as calculated for the MB dye degradation employing ZnO NPs is $5.175 \times 10^{-2}$.This reflects that the synthesized ZnO NPs degraded MB dye more efficiently[53].

**Table1** Kinetics of the degradation of MB dye over BC-ZnO NPs as photocatalyst

| Type of nanocatalyst | Rate constant ($min^{-1}$) | Correlation coefficient ($R^2$) | Percent degradation in 90 minutes | Half-Life period |
|---|---|---|---|---|
| BC-ZnO NPs | $5.175 \times 10^{-2}$ | 0.98594 | 99 | 13.3913 |

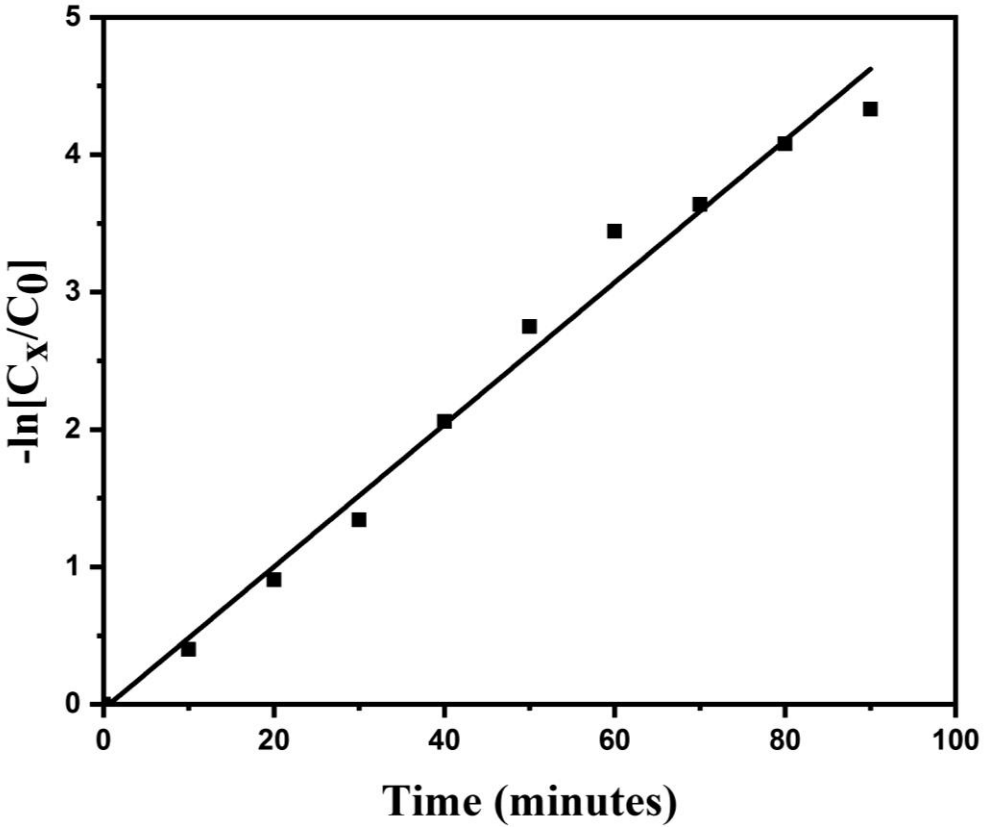


**Fig.10** Degradation Kinetic Study of BC-ZnO NPs

The linear trend indicates that the degradation process adheres topseudo-first-order kinetics, which is typically seen in photocatalytic reactions when the dye concentration is low and active sites on the catalyst surface are in excess[55]. The relatively higher rate constant (0.05175 $min^{-1}$) suggests efficient degradation.In studies involving ZnO nanoparticles as photocatalysts for dye

degradation, typical (pseudo-first-order) rate constants fall in the range of 0.01–0.05 $min^{-1}$, depending on: particle size and morphology, light source and intensity, dye concentration and type and catalyst dosage[56–58].

### 3.6.Biological activities of BC-ZnO NPs

#### 3.6.1. Antioxidant activity

The antioxidant potency of the ZnO NPs mediated by *B. ceiba* flower petals' extractwas studied using DPPH assays. In the DPPH assay, at 100µg/mL, BC-ZnO NPs exhibited antioxidant activity at 38.87%.Notably, the scavenging activity of ZnO NPs is dose-dependent, and its percentage increases with increasing concentration. The lower $IC_{50}$ value (46.34µg/mL) indicated the superior antioxidant capacity of ZnO NPs. The promising results of our inquiry provide a basis for further exploration into green-produced ZnO NPs as a viable antioxidant option.

#### 3.6.2. Antidiabetic activity

The two digestive tract enzymes that catalyze starch breakdown and subsequent monosaccharides'production are α- glucosidase and α- amylase.In the present study, the antidiabetic potency of BC-ZnO NPs was examined through the inhibition of α-amylase and α-glucosidase. The antidiabetic study's findings (Table 2) revealed good inhibition activity against α-amylase and α glucosidase. For the α-amylase, 24.46%($IC_{50}$ value 119.95 µg/mL) inhibition activity at the concentration of 500 µg/mL compared to the standard ($IC_{50}$ value 1.22 µg/mL) whereas for α-glucosidase, BC-ZnO NPs exhibited 36.39% ($IC_{50}$value 98.94 µg/mL) inhibition activity at 500 µg/mL concentration,which explored good efficiency compared to standard Acarbose ($IC_{50}$ value 0.24 µg/mL). Consequently, the exceptional ability of ZnO NPs to inhibit α-amylase and α-glucosidase, as demonstrated in the outcomes above, indicates their efficacy in managing diabetes.

**Table2**-Showing antioxidant and antidiabetic activity with $IC_{50}$ value of BC-ZnO NPs in *in vitro* α-amylase & α-glucosidase

| **Compounds name** | **Antidiabetic activity** | | **Antioxidant activity** |
|---|---|---|---|
| | **$IC_{50}$ (α-amylase)** | **$IC_{50}$ (α-glucosidase)** | |
| **ZnO NPs** | 119.95 | 98.94 | 46.34 |
| **Standard** | 2.11 | 0.24 | - |

### 3.6.3. Antimicrobial activity

Using the standard Agar Well Diffusion method, synthesized ZnO NPs were screened against *S. aureus* &*E. coli* (bacterial strains) and *C. albicans* (fungal strain). Ciprofloxacin and Ketoconazole are standard antibiotics for antibacterial and antifungal activity, respectively. Fig.11shows maximum inhibition activity and antimicrobial activity of BC-ZnO NPs. These NPs exhibited good efficacy against *C. albicans* but were less effective against both bacterial strains.Outcomes of this study are shown in Table 3.

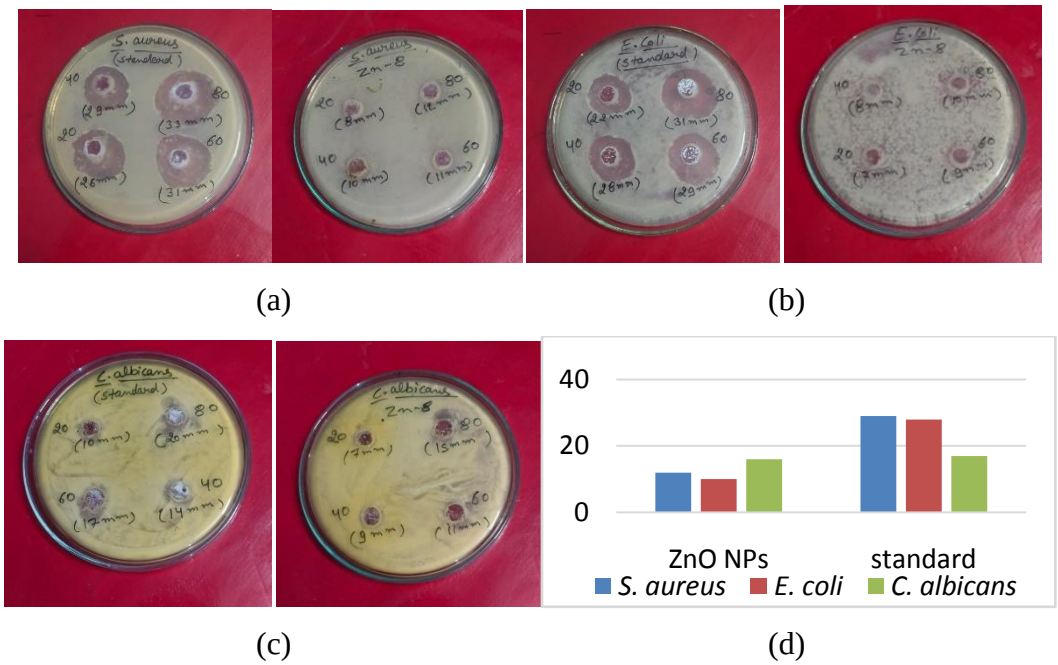


**Fig.11**Antimicrobial activity of BC-ZnO NPs against (a) *S. aureus* (b) *E. coli* (c) *C. albicans* (d) bar diagram of antimicrobial activity showing maximum inhibition activity (in mm diameter)

**Table 3** Antimicrobial activity (inhibition zone in mm diameters) of BC-ZnO NPs

| **Compound name** | **Bacterial strain** | | **Fungal strain** |
|---|---|---|---|
| | **Gram +ve** | **Gram -ve** | |
| | ***S. aureus*** | ***E. coli*** | ***C. albicans*** |
| | 20 40 60 80 ( µg/mL ) | 20 40 60 80 ( µg/mL ) | 20 40 60 80 ( µg/mL ) |

| | | | |
|---|---|---|---|
| **BC-ZnO NPs** | 08 10 11 12 | 07 08 09 10 | 07 09 11 15 |
| **Ciprofloxacine** | 29 | 28 | |
| **Ketoconazole** | | | 17 |

In the present investigation, it is found that ZnO NPs exhibited 12 and 10 mm (zone of inhibition), against *S. aureus* and *E. coli*, in comparison to the standard (29 and 28 mm) and 15 mm against the *C. albicans* which is closer to the standard (17 mm).The ZnO NPs exhibit antibacterial activity because of the permutation of numerous aspects, like their interaction with bacterial cell walls, disruption of membrane integrity, generation of reactive oxygen species (ROS), and the release of zinc ions. The ROS penetrate the bacterial membrane and contribute to cellular damage, ultimately leading to bacterial cell death.

## Conclusions

This paper reports the biosynthesis of zinc oxide nanoparticles employing Bombax ceiba flower petals' extract. The PXRD pattern confirms highly crystalline ZnO nanoparticles in a wurtzite hexagonal phase. BC-ZnO NPs with an average size of ~41.89 nm was obtained. BC-ZnO NPs displayed a prominent absorbance at 356nm in UV–Visible spectra and a wide band gap (3.23 eV).The FESEM images revealed the flake-like or petal-shaped appearance of the particles, giving a flower-like or agglomerated granular morphology. The photocatalytic efficiency of the reported BC-ZnO NPs was assessed against MB dye. These NPs exhibited ~90% photodegradation during the initial 40 min and ~ 99% in 80 min of UV light irradiation.

Further, prepared NPs were examined for their antimicrobial, antioxidant, and antidiabetic activities. The BC-ZnO NPs ($IC_{50}$ value 119.95 µg/mL) showed good antidiabetic activity (α-amylase activity) as compared to the standard ($IC_{50}$ value 2.11 µg/mL). For α-glucosidase, BC-ZnO NPs ($IC_{50}$ value 98.94 µg/mL) exhibited good inhibition activity compared to the standard Acarbose ($IC_{50}$ value 0.24 µg/mL). The lower $IC_{50}$ value (46.34 µg/mL) of the BC-ZnO NPs was represented as their excellent antioxidant capability. Regarding Antimicrobial activity, BC-ZnO NPs exhibited good efficacy against fungal strains (*C. albicans*) and bacterial strains (*S. aureus* &*E. coli*). In addition to antidiabetic and antimicrobial uses, the excellent potency of ZnO NPs against antioxidant is a positive symbol of its effectiveness in antioxidant treatment, thereby making these green synthesized ZnO NPs, a helpful candidate for biomedical applications.

Overall BC-ZnO NPs can prove quite useful for photocatalytic and gas-sensing abilities,and other biological applications.

**Acknowledgement** The authors are highly thankful to the department of Chemistry, BMU Asthal Bohar, Rohtak for providing the research facility.

**Competing interests** None.

**Funding**None

**References**

1. Azanaw A, Birlie B, Teshome B, Jemberie M (2022) Textile effluent treatment methods and eco-friendly resolution of textile wastewater. Case Studies in Chemical and Environmental Engineering 6:100230. https://doi.org/10.1016/j.cscee.2022.100230

2. University of Novi Sad, Faculty of Sciences, Department of Chemistry, Biochemistry and Environmental Protection, Novi Sad, Serbia, Kerkez Đ, Bečelić-Tomin M, et al (2020) Treatment of wastewater containing printing dyes: summary and perspectives. In: Proceedings - The Tenth International Symposium GRID 2020. University of Novi Sad, Faculty of technical sciences, Department of graphic engineering and design, pp 289–295

3. Anjum M, Miandad R, Waqas M, et al (2019) Remediation of wastewater using various nano-materials. Arabian Journal of Chemistry 12:4897–4919. https://doi.org/10.1016/j.arabjc.2016.10.004

4. Zelekew OA, Haitosa HH, Chen X, Wu Y-N (2023) Recent progress on plant extract-mediated biosynthesis of ZnO-based nanocatalysts for environmental remediation: Challenges and future outlooks. Advances in Colloid and Interface Science 317:102931. https://doi.org/10.1016/j.cis.2023.102931

5. Lu H, Wang J, Stoller M, et al (2016) An Overview of Nanomaterials for Water and Wastewater Treatment. Advances in Materials Science and Engineering 2016:1–10. https://doi.org/10.1155/2016/4964828

6. Mittal A, Sharma S, Kumari V, et al (2019) Highly efficient, visible active TiO2/CdS/ZnS photocatalyst, study of activity in an ultra low energy consumption LED based photo reactor. J Mater Sci: Mater Electron 30:17933–17946. https://doi.org/10.1007/s10854-019-02147-6

7. Karthikeyan C, Arunachalam P, Ramachandran K, et al (2020) Recent advances in semiconductor metal oxides with enhanced methods for solar photocatalytic applications. Journal of Alloys and Compounds 828:154281. https://doi.org/10.1016/j.jallcom.2020.154281

8. Al-Mohaimeed AM, Al-Onazi WA, El-Tohamy MF (2022) Multifunctional Eco-Friendly Synthesis of ZnO Nanoparticles in Biomedical Applications. Molecules 27:579. https://doi.org/10.3390/molecules27020579

9. Naiel B, Fawzy M, Halmy MWA, Mahmoud AED (2022) Green synthesis of zinc oxide nanoparticles using Sea Lavender (Limonium pruinosum L. Chaz.) extract: characterization, evaluation of anti-skin cancer, antimicrobial and antioxidant potentials. Sci Rep 12:20370. https://doi.org/10.1038/s41598-022-24805-2

10. Saha R, Subramani K, Sikdar S, et al (2021) Effects of processing parameters on green synthesised ZnO nanoparticles using stem extract of Swertia chirayita. Biocatalysis and Agricultural Biotechnology 33:101968. https://doi.org/10.1016/j.bcab.2021.101968

11. Hessien M (2022) Recent progress in zinc oxide nanomaterials and nanocomposites: From synthesis to applications. Ceramics International 48:22609–22628. https://doi.org/10.1016/j.ceramint.2022.05.082

12. Alvi GB, Iqbal MS, Ghaith MMS, et al (2021) Biogenic selenium nanoparticles (SeNPs) from citrus fruit have antibacterial activities. Sci Rep 11:4811. https://doi.org/10.1038/s41598-021-84099-8

13. Waqas M, Aslam S, Akram M, et al (2022) Bombax Ceiba Flower Extract Induced Surface Groups on Se Nanoparticles to Enhance Antibacterial Activity and Urea Detection

14. Mekuye B, Abera B (2023) Nanomaterials: An overview of synthesis, classification, characterization, and applications. Nano Select 4:486–501. https://doi.org/10.1002/nano.202300038

15. Singh P, Kim Y-J, Zhang D, Yang D-C (2016) Biological Synthesis of Nanoparticles from Plants and Microorganisms. Trends in Biotechnology 34:588–599. https://doi.org/10.1016/j.tibtech.2016.02.006

16. Iravani S (2011) Green synthesis of metal nanoparticles using plants. Green Chem 13:2638. https://doi.org/10.1039/c1gc15386b

17. Patra JK, Baek K-H (2014) Green Nanobiotechnology: Factors Affecting Synthesis and Characterization Techniques. Journal of Nanomaterials 2014:417305. https://doi.org/10.1155/2014/417305

18. Negash A, Mohammed S, Weldekirstos HD, et al (2023) Enhanced photocatalytic degradation of methylene blue dye using eco-friendly synthesized rGO@ZnO nanocomposites. Sci Rep 13:22234. https://doi.org/10.1038/s41598-023-48826-7

19. (2025) Energy-efficient synthesis of ZnO nanoparticles using White Ash Gourd Fruit Extract for their medicinal and environmental applications. IJC 64:. https://doi.org/10.56042/ijc.v64i1.13833

20. Abd-Elhaki MM, Ahmed El-B N, Kamal Eldi E, et al (2019) Protective and Curative Effects of Bombax ceiba Flower and Ziziphus spina christi Fruit Extracts on Gastric Ulcer. J of Biological Sciences 19:161–172. https://doi.org/10.3923/jbs.2019.161.172

21. Das G, Shin H-S, Ningthoujam SS, et al (2021) Systematics, Phytochemistry, Biological Activities and Health Promoting Effects of the Plants from the Subfamily Bombacoideae (Family Malvaceae). Plants 10:651. https://doi.org/10.3390/plants10040651

22. Saleem R, Ahmad M, Hussain SA, et al (1999) Hypotensive, Hypoglycaemic and Toxicological Studies on the Flavonol C-Glycoside Shamimin from Bombax ceiba. Planta med 65:331–334. https://doi.org/10.1055/s-1999-14060

23. Mane RS, Vedamurthy AB (2020) CRITICAL REVIEW ON BOMBAX CEIBA, ALOE VERA AND XIMENIA AMERICANA. Univ J Pharm Res. https://doi.org/10.22270/ujpr.v5i2.392

24. Chaudhary P, Khadabadi S (2012) Bombax ceiba Linn.: Pharmacognosy, Ethnobotany and Phyto-pharmacology. Phcog Commn 2:02–09. https://doi.org/10.5530/pc.2012.3.2

25. Joshi KR, Devkota HP, Yahara S (2013) Chemical Analysis of Flowers of *Bombax ceiba* from Nepal. Natural Product Communications 8:1934578X1300800508. https://doi.org/10.1177/1934578X1300800508

26. (2023) Phytochemical Constituent Analysis, Antioxidative Effect, and Anti-inflammatory Activity of Bombax ceiba Flowers. Biointerface Res Appl Chem 13:408. https://doi.org/10.33263/BRIAC135.408

27. Chakraborty DD, V R, Chakraborty P PHYTOCHEMICAL EVALUATION AND TLC PROTOCOL OF VARIOUS EXTRACTS OF BOMBAX CEIBA LINN. http://dx.doi.org/10.13040/IJPSR.0975-8232.1(8-S).66-73

28. Sharma S, Thakur R, Mishra R, Sharma B BOMBAX CEIBA: A PLANT OF THERAPEUTIC POTENTIAL. https://doi.org/10.13040/IJPSR.0975-8232.16(3).591-600

29. Meena PL, Poswal K, Surela AK (2022) Facile synthesis of ZnO nanoparticles for the effective photodegradation of malachite green dye in aqueous solution. Water & Environment J 36:513–524. https://doi.org/10.1111/wej.12783

30. Mohammed R, Ali MEM, Gomaa E, Mohsen M (2020) Green ZnO nanorod material for dye degradation and detoxification of pharmaceutical wastes in water. Journal of Environmental Chemical Engineering 8:104295. https://doi.org/10.1016/j.jece.2020.104295

31. Kumari V, Yadav S, Mittal A, et al (2020) Hydrothermally synthesized nano-carrots ZnO with CeO2 heterojunctions and their photocatalytic activity towards different organic pollutants. J Mater Sci: Mater Electron 31:5227–5240. https://doi.org/10.1007/s10854-020-03083-6

32. Dadi R, Azouani R, Traore M, et al (2019) Antibacterial activity of ZnO and CuO nanoparticles against gram positive and gram negative strains. Materials Science and Engineering: C 104:109968. https://doi.org/10.1016/j.msec.2019.109968

33. Ahmed HE, Iqbal Y, Aziz MH, et al (2021) Green Synthesis of CeO2 Nanoparticles from the Abelmoschus esculentus Extract: Evaluation of Antioxidant, Anticancer, Antibacterial, and Wound-Healing Activities. Molecules 26:4659. https://doi.org/10.3390/molecules26154659

34. Iqbal Y, Raouf Malik A, Iqbal T, et al (2021) Green synthesis of ZnO and Ag-doped ZnO nanoparticles using Azadirachta indica leaves: Characterization and their potential antibacterial, antidiabetic, and wound-healing activities. Materials Letters 305:130671. https://doi.org/10.1016/j.matlet.2021.130671

35. Gonz 醢 ez-Fern 酱 dez J, David Pinz 髇-Moreno D, Alexander Neciosup-Puican A, Ver 髇 ica Carranza-Oropeza M (2022) Green Method, Optical and Structural Characterization of ZnO Nanoparticles Synthesized Using Leaves Extract of M. oleifera. Journal of Renewable Materials 10:833–847. https://doi.org/10.32604/jrm.2022.017377

36. Alhudhaibi AM, Ragab SM, Sharaf M, et al (2024) Effect of *ex situ* , eco-friendly ZnONPs incorporating green synthesised *Moringa oleifera* leaf extract in enhancing biochemical and molecular aspects of *Vicia faba* L. under salt stress. Green Processing and Synthesis 13:20240012. https://doi.org/10.1515/gps-2024-0012

37. Rajkumari NP, Rouf A, Dutta P, Goswami P (2023) Synchronizing charge-carrier capacity and interfacial morphology of green rGO modified ZnO and TiO2 heterojunctions and study of their photocatalytic behaviour towards UV and visible light active drug and dye. Materials Science and Engineering: B 287:116094. https://doi.org/10.1016/j.mseb.2022.116094

38. Srikant V, Clarke DR (1998) On the optical band gap of zinc oxide. Journal of Applied Physics 83:5447–5451. https://doi.org/10.1063/1.367375

39. Haryński Ł, Olejnik A, Grochowska K, Siuzdak K (2022) A facile method for Tauc exponent and corresponding electronic transitions determination in semiconductors directly from UV–Vis spectroscopy data. Optical Materials 127:112205. https://doi.org/10.1016/j.optmat.2022.112205

40. Dhivya Ponnusamy, Sridharan Madanagurusamy (2014) Nanostructured ZnO Films for Room Temperature Ammonia Sensing. Journal of Elec Materi 43:3211–3216. https://doi.org/10.1007/s11664-014-3253-8

41. Molefe FV, Koao LF, Dejene BF, Swart HC (2015) Phase formation of hexagonal wurtzite ZnO through decomposition of Zn(OH)2 at various growth temperatures using CBD method. Optical Materials 46:292–298. https://doi.org/10.1016/j.optmat.2015.04.034

42. Sedefoglu N (2023) Characterization and photocatalytic activity of ZnO nanoparticles by green synthesis method. Optik 288:171217. https://doi.org/10.1016/j.ijleo.2023.171217

43. Meena PL, Poswal K, Surela AK (2022) Facile synthesis of ZnO nanoparticles for the effective photodegradation of malachite green dye in aqueous solution. Water & Environment J 36:513–524. https://doi.org/10.1111/wej.12783

44. Li B, Wang Y (2010) Facile synthesis and photocatalytic activity of ZnO–CuO nanocomposite. Superlattices and Microstructures 47:615–623. https://doi.org/10.1016/j.spmi.2010.02.005

45. Elbrolesy A, Abdou Y, Elhussiny FA, Morsy R (2023) Novel Green Synthesis of UV-Sunscreen ZnO Nanoparticles Using Solanum Lycopersicum Fruit Extract and Evaluation of Their Antibacterial and Anticancer Activity. J Inorg Organomet Polym 33:3750–3759. https://doi.org/10.1007/s10904-023-02744-3

46. De Peres ML, Delucis RDA, Amico SC, Gatto DA (2019) Zinc oxide nanoparticles from microwave-assisted solvothermal process: Photocatalytic performance and use for wood protection against xylophagous fungus. Nanomaterials and Nanotechnology 9:184798041987620. https://doi.org/10.1177/1847980419876201

47. Thongam DD, Gupta J, Sahu NK (2019) Effect of induced defects on the properties of ZnO nanocrystals: surfactant role and spectroscopic analysis. SN Appl Sci 1:1030. https://doi.org/10.1007/s42452-019-1058-3

48. Lal R, Gour T, Dave N, et al (2024) Green route to fabrication of Semal-ZnO nanoparticles for efficient solar-driven catalysis of noxious dyes in diverse aquatic environments. Front Chem 12:1370667. https://doi.org/10.3389/fchem.2024.1370667

49. Abdullah JAA, Rosado MJ, Guerrero A, Romero A (2023) Eco-friendly synthesis of ZnO-nanoparticles using *Phoenix dactylifera* L., polyphenols: physicochemical, microstructural, and functional assessment. New J Chem 47:4409–4417. https://doi.org/10.1039/D3NJ00131H

50. Chabou N, Birouk B, Aida MS, Raskin JP (2020) Deposition time and annealing effects on morphological and optical properties of ZnS thin films prepared by chemical bath deposition. Materials Science-Poland 38:508–517. https://doi.org/10.2478/msp-2020-0052

51. Raj VJ, Ghosh R, Girigoswami A, Girigoswami K (2022) Application of zinc oxide nanoflowers in environmental and biomedical science. BBA Advances 2:100051. https://doi.org/10.1016/j.bbadva.2022.100051

52. Dao TT, Le Na Vo T, Duong AT, et al (2023) Highly photocatalytic activity of pH-controlled ZnO nanoflakes. Optical Materials 140:113865. https://doi.org/10.1016/j.optmat.2023.113865

53. Venkatesan S, Suresh S, Arumugam J, et al (2024) Sunlight assisted degradation of methylene blue dye by zinc oxide nanoparticles green synthesized using Vitex negundo plant leaf extract. Results in Chemistry 7:101315. https://doi.org/10.1016/j.rechem.2024.101315

54. Mittal A, Sharma S, Kumar T, et al (2020) Surfactant-assisted hydrothermally synthesized novel TiO2/SnS@Pd nano-composite: structural, morphological and photocatalytic activity. J Mater Sci: Mater Electron 31:2010–2021. https://doi.org/10.1007/s10854-019-02720-z

55. Matinise N, Botha N, Fall A, Maaza M (2025) Enhanced photocatalytic degradation of methylene blue using zinc vanadate nanomaterials with structural and electrochemical properties. Sci Rep 15:26333. https://doi.org/10.1038/s41598-025-11418-8

56. Modi S, Yadav VK, Amari A, et al (2023) Photocatalytic Degradation of Methylene Blue Dye from Wastewater by Using Doped Zinc Oxide Nanoparticles. Water 15:2275. https://doi.org/10.3390/w15122275

57. Atta D, Wahab HA, Ibrahim MA, Battisha IK (2024) Photocatalytic degradation of methylene blue dye by ZnO nanoparticle thin films, using Sol–gel technique and UV laser irradiation. Sci Rep 14:26961. https://doi.org/10.1038/s41598-024-76938-1

58. Yang C, Wang X, Ji Y, et al (2019) Photocatalytic degradation of methylene blue with ZnO@C nanocomposites: Kinetics, mechanism, and the inhibition effect on monoamine oxidase A and B. NanoImpact 15:100174. https://doi.org/10.1016/j.impact.2019.100174